Adv. Geosci., 24, 69–82, 2010
www.adv-geosci.net/24/69/2010/

Advances in Geosciences

Integration of ground-penetrating radar, ultrasonic tests and infrared thermography for the analysis of a precious medieval rose window

L. Nuzzo[1], **A. Calia**[2], **D. Liberatore**[3], **N. Masini**[4], **and E. Rizzo**[5]

[1]Ingegneria dei Sistemi LTD – IDS (UK), Fareham, Hampshire, UK
[2]Istituto Beni Archeologici e Monumentali, IBAM-CNR, Lecce, Italy
[3]Dipartimento di Ingegneria Strutturale e Geotecnica, University of Rome "La Sapienza", Italy
[4]Istituto Beni Archeologici e Monumentali, IBAM-CNR, Tito Scalo (PZ), Italy
[5]Istituto di Metodologie per l'Analisi Ambientale, IMAA-CNR, Tito Scalo (PZ), Italy

Received: 20 November 2009 – Revised: 18 January 2010 – Accepted: 30 January 2010 – Published: 15 April 2010

Abstract. The integration of high-resolution, non-invasive geophysical techniques (such as ground-penetrating radar or GPR) with emerging sensing techniques (acoustics, thermography) can complement limited destructive tests to provide a suitable methodology for a multi-scale assessment of the state of preservation, material and construction components of monuments. This paper presents the results of the application of GPR, infrared thermography (IRT) and ultrasonic tests to the 13th century rose window of Troia Cathedral (Apulia, Italy), affected by widespread decay and instability problems caused by the 1731 earthquake and reactivated by recent seismic activity. This integrated approach provided a wide amount of complementary information at different scales, ranging from the sub-centimetre size of the metallic joints between the various architectural elements, narrow fractures and thin mortar fillings, up to the sub-metre scale of the internal masonry structure of the circular ashlar curb linking the rose window to the façade, which was essential to understand the original building technique and to design an effective restoration strategy.

1 Introduction

The correct management and restoration of architectural monuments of high cultural interest requires a comprehensive understanding of their state of preservation, the detection of the building features, the localization of damages and possibly the identification of their causes, nature and extent. Since for obvious reasons destructive tests must be restricted to a few locations of the investigated structure, in recent times there is a growing interest on non-destructive and non-invasive geophysical methods as an invaluable tool for correlating spatially the information gained through destructive tests and to optimize their location in order to minimize their impact on the monument. Moreover, the integration of classical geophysical techniques, such as ground-penetrating radar (GPR), with emerging surface and subsurface sensing techniques (acoustics, infrared thermography) provides a suitable methodology for a multi-scale assessment of the monument state of preservation and its material and building components, which is essential to address maintenance and restoration issues. Since the various non-destructive techniques (NDT) are based on different theoretical principles and provide information regarding different physical parameters of the structure, the choice the NDT method(s) best suited for studying a particular structural problem depends upon the physical properties of the construction materials which offer the best chance of being reliably determined. A useful review of geophysical and NDT methods for the assessment of masonry structures and a summary of their basic principles can be found in Flint et al. (1999) and McCann and Forde (2001). Previous studies have shown the potential of the above techniques to cast light on some important aspects of cultural heritage preservation. GPR has been frequently used for investigating masonry structures (Binda et al., 1998; Maierhofer and Leipold, 2001; Ranalli et al., 2004; Binda et al., 2005; Masini et al., 2010) as well as for characterizing the foundation subsoil and locating archaeological remains, occasionally in conjunction with other geophysical, physical and biological techniques (Cardarelli et al., 2002; Cataldo et al., 2005; Nuzzo et al., 2009). The use of sonic

Correspondence to: L. Nuzzo
(l.nuzzo@idsuk-ltd.co.uk)

Published by Copernicus Publications on behalf of the European Geosciences Union.

techniques for cultural heritage and civil engineering applications is also well documented (Colla et al., 1997; Binda et al., 2001, 2003a, b) whereas ultrasonic tests are less frequent. Infrared thermography (IRT) is an efficient investigative tool used for more than 30 years in the inspection and diagnosis of modern and historic buildings (Titman, 2001; Clark et al., 2003) to detect shallow subsurface voids and defects (Inagaki et al., 1999; Maierhofer et al., 2003), to map moisture (Grinzato et al., 2002) and to evaluate conservation treatments (Avdewlidis and Moropolou, 2004). Although in most studies presented in the literature only one or two techniques are employed, for monuments of exceptional artistic value or high structural-compositional complexity, the integration of several methods becomes mandatory in order to reduce interpretation ambiguities and the risk of failure in detecting structural defects. In our case the multiplicity and complexity of issues to be addressed required an integrated and multi-scale NDT approach (Liberatore et al., 2006; Nuzzo et al., 2008) to complement the laboratory analyses for material characterization.

2 Brief description of the NDT methods

The present case study focuses on the application of GPR, ultrasonic tests and IRT to analyze a 13th century precious rose window in Southern Italy, affected by widespread decay and instability problems. The combination of GPR, IRT and sonic/ultrasonic tests was deemed the best strategy to exploit their ability to provide information on different physical parameter and to achieve different depths of penetration and resolution capabilities. In this paragraph the basic principles of the methods employed are briefly recalled.

2.1 Ground penetrating radar

Ground Penetrating Radar is based on the propagation of electromagnetic (EM) waves inside the subsurface and their reflection at interfaces separating media with contrasting EM properties (typically different values of the dielectric constant). An antenna pair (with nominal frequency typically in the 100–2000 MHz range) sends short EM pulses into the subsurface and records the returning echoes. After estimating the subsurface propagation velocity (from diffraction hyperbolas or from the two-way travel time to reflectors at known depths) the (time-distance) radargram can be converted into a depth-distance cross-section of the investigated medium along the surveyed profile. By collecting several (parallel) profiles and using advanced processing and visualization methods (Nuzzo et al., 2002) it is possible to obtain three-dimensional images of the investigated area. More sophisticated analyses of the reflected amplitudes can provide information on the reflection/attenuation properties of the probed material and give further insights into its physical characteristics. The main limit of GPR is the high absorption of the EM energy in conductive (moist) materials that considerably reduces its penetration depth.

2.2 Sonic and ultrasonic tests

Sonic and ultrasonic techniques are based on the transmission/reflection of acoustic waves inside the investigated medium to inspect civil engineering structures and building materials. Typical frequencies are 10^2–10^4 Hz for the sonic and 10^4–10^6 Hz for the ultrasonic tests. The ultrasonic reflection method (based on the same principle of GPR but using a different wave-field and instrumentation) uses a piezoelectric transducer above 20 kHz to generate high frequency ultrasonic energy and investigate the presence of subsurface discontinuities (such as cracks), reflecting back part of the energy. Signal travel times can be directly related to the reflector distance. Reflection ultrasonic inspection is widely used for flaw detection/evaluation, dimensional measurements and material characterization. However, in the investigation of masonry structures the high attenuation/scattering due to material heterogeneity can limit the penetration depth and the poor coupling on rough surfaces can cause a low signal to noise ratio. Direct transmission method involves the transmission of a pressure wave through the structure from a source (hammer for the sonic, piezoelectric transmitter for the ultrasonic) to a sensor (accelerometer or piezoelectric receiver) located on the opposite side of the structure directly in front of the source point. The resulting wave velocity is an average of the local velocity along the path and can be plotted in a contour map format to allow a simple evaluation of the relative internal condition of the structure and a semi-quantitative assessment of its mechanical properties.

2.3 Infrared thermography

Infrared thermography is a remote sensing method based on the property that all objects above 0 K emit infrared (IR) radiation, i.e. electromagnetic energy in the 10^{12}–10^{14} Hz band of the EM spectrum. Using a suitable IR device (IR camera) it is possible to measure this energy and to retrieve the temperature distribution on the object surface by means of the Stefan-Boltzmann law. Abnormal surface temperature profiles are often an important indication of potential subsurface problems. The energy emitted by the surface depends on the spectral (emissivity, reflection), thermal (conductivity, specific heat, diffusivity) and other physical properties of the underlying material (porosity, density, water content). Therefore, the interpretation of IR images is not an easy task and in the inspection and diagnosis of historic buildings this technique is generally used as an economical, efficient, non-destructive tool for qualitative detection of shallow subsurface voids and defects, to map moisture and to evaluate conservation treatments. Passive thermography exploits the property that the features of interest have naturally higher

or lower temperature than the background (e.g. in people surveillance or medical diagnosis) whereas active thermography is used in applications where the features of interest are normally in thermal equilibrium with the surroundings and an energy source is required to enhance the thermal contrast.

3 Historical and architectural background

The Cathedral of Troia (Apulia, Italy) was built between 1093 and 1120 AD and is the masterpiece of the Apulian Romanesque architecture, blending Byzantine and Muslim reminiscences with oriental elements (Belli D'Elia, 1998). It has a Latin cross plan with three naves separated by two rows of 6 columns and a 13th column at the side of the first column on the right. The recurrence of particular numbers, geometrical shapes and figurative elements is a peculiarity of this extraordinary architectural building with strong and sometimes enigmatic Christian symbolism. Its façade (Fig. 1a) is 18.28 m wide and 19.90 m high. The basement is decorated with seven blind arches, rhombi and oeil-de-boeufs characterized by chiaroscuro effects through the use of the whitish calcarenite of Castelluccio and the greenish sandstone of Roseto. The central tympanum consists of two round arches: the external arch rests on two couples of columns in reused marble supported by lion statues, the internal arch is richly sculptured with geometric, phytomorphic, zoomorphic and anthropomorphic elements and bas-relief. Inside this arch there is the rose window (Fig. 1b). It has a 6 m diameter and consists of 11 twin columns, external and internal, in stone and reused marble, connected to a central oculus and to a ring of trapezoidal elements decorated with arched ribworks forming ogives. Between the twin columns there are 11 triangular carved panels with different and strongly symbolic geometrical patterns (square, rhomb, cross and circle). As a consequence of the 1731 earthquake, the upper part of the façade underwent rotational strains which induced severe out-of-plane deformation in the rose window and caused disconnection and rotation of the capitals, as well as compression failures, cracks and detachments in other architectural elements. A previous ambient vibration survey permitted to identify the eigenfrequencies of the first in-plane and out-of-plane modes of the façade and the first out-of-plane mode of the rose window (Liberatore et al., 2006). In the late 19th century some metallic bars (black in Fig. 1b) and two tie-beams were inserted to consolidate the structure. Unfortunately, recent seismic activity determined an increase of the compressional-rotational strains and made necessary further structural rehabilitation works to preserve the historical rose window.

4 Methodology

To identify the most effective restoration procedure a multi-technique NDT approach was chosen as a support to direct investigations in order to formulate a correct diagnosis of the problems and achieve an accurate knowledge of the building internal structure and state of preservation.

4.1 Analysis of building materials

Visual inspection, mineralogical and petrographical studies based on optical microscopy observations of thin sections in polarized light and X-rays diffractometry (XRD) analyses were performed for the identification of the building materials. According to these studies different materials have been used for the realisation of various architectural elements (Figs. 1c, d and 2).

The central oculus is made of a fine-grained compact limestone. According to Dunham, 1962 and Folk, 1959, its petrographical classification corresponds to a wackestone or biomicrite. The carved triangular panels, the interlacing arches and the capitals of the columns are composed of bioclastic calcarenites. They differ in terms of granulometry, degree of compactness and cementation, diagenetic features. Medium to coarse-grained varieties constitute the panels and the arches, while medium-finer ones are used for the realisation of the capitals. Their petrographical classification range from packstones to grainstones (or biosparite). The petrographic features of these stones allow to suppose a provenance from the near Appenninic and Gargano geological area. XRD analyses carried out on the samples of limestones and calcarenites give the calcite as the main mineralogical component, sometime with traces of quartz, already observed as small grains by optical microscopy.

Different varieties of stones constitute the columns of the rose window. The visual inspection reveals the presence of some kinds of marbles, including marbles *sinsu strictu* in geological terms and ornamental stones generally named "Marmora" in the ancient time (Gnoli, 1971; Borghini, 1989). Ultrapure white marbles, with grey stripes or grey spots, whose identification needs specific and combined analyses, have been recognized as Proconnesian (coming from Marmara Island, Turkey), Parian (coming from Paros Island, Greece) and Carrara marbles, on the basis of their petrographic features and isotopic composition (Calia et al., 2006). Coloured marbles such as white marble breccia with purple matrix ("Pavonazzetto"), calcareous breccia with a reddish ferruginous-clayey matrix ("Breccia corallina") – both of Turkish provenance – or with brown-greyish matrix have been identified by visual inspection. White and coloured marbles are mostly reused marbles coming from the ancient Aecae, a Roman site located near Troia, according to the common practice of re-using architectural elements taken from ancient monuments along the Middle Age, as well as during Byzantine centuries. Other stones such

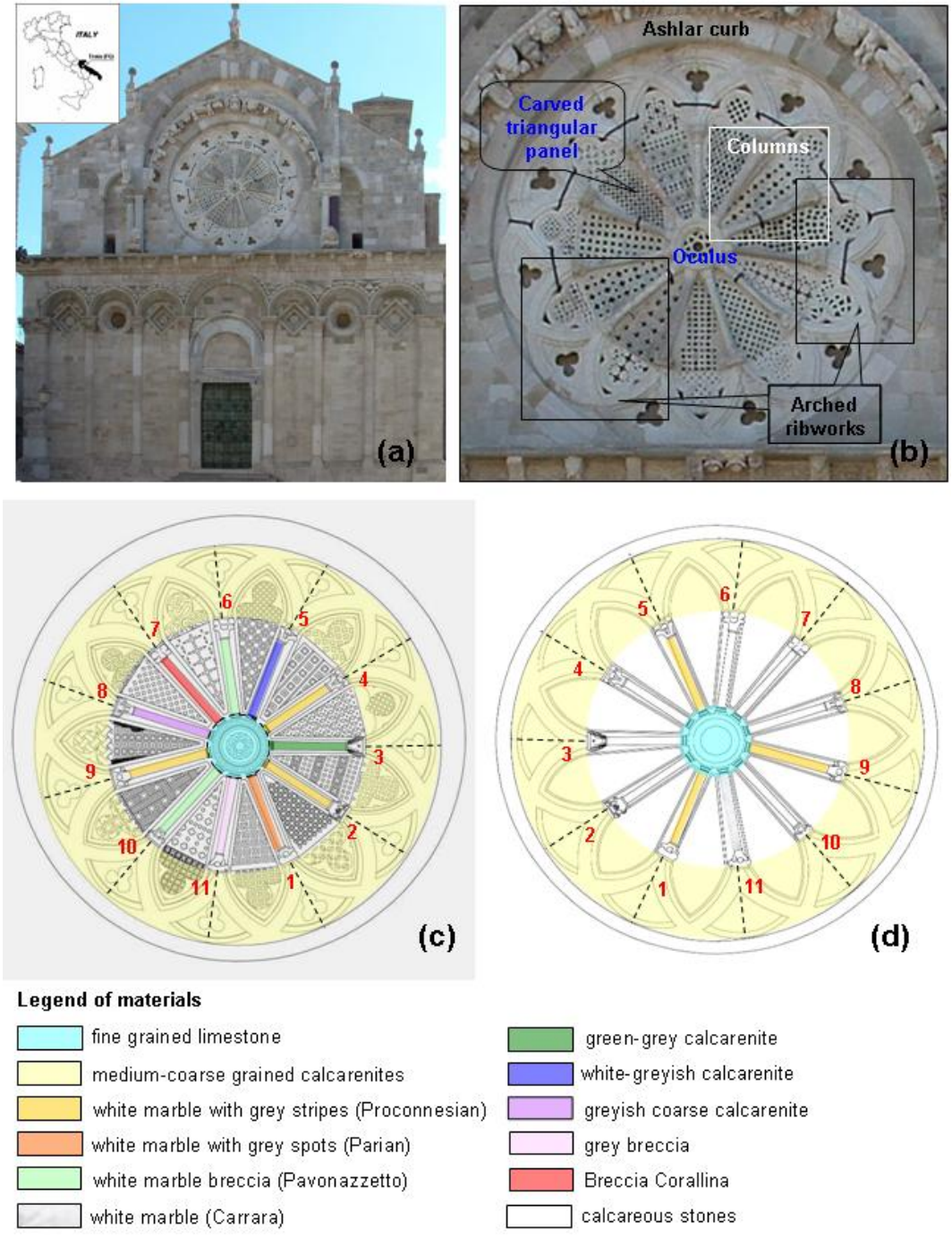

Fig. 1. (a) Façade and **(b)** rose window of Troia Cathedral (Apulia, Italy). **(c)** External and **(d)** internal building materials.

as white-greyish calcarenite, coarse greyish calcarenite and green-grey calcarenite are employed as constituent materials of some external columns. Optical microscopy observations reveal that the white-greyish calcarenite is a very well cemented packstone, while the greenish calcarenite shows a high degree of compactness and an abundant amount of glauconite. Calcareous stones have also been macroscopically observed as constituent materials of some internal columns. Finally, the ashlar curb consists of two main kinds of materials, light-coloured calcarenites and greenish sandstones, the latter showing the same characteristics that have been previously described. Their provenance is supposedly from

Fig. 2. Examples of building materials used for columns (grey breccia, Pavonazzetto marble, Breccia Corallina and green-grey sandstone), capitals (medium-fine grained calcarenites), arched ribworks and triangular carved panels (medium to coarse grained calcarenites).

quarries located in the territories of two neighbouring villages, Castelluccio Valmaggiore and Roseto Valfortore, according to the similarities of the curb materials with rock samples from the supposed origins.

Because of the different nature and composition of the constituent stone materials, different responses to the electromagnetic and ultrasonic investigation were therefore expected. The various elements are supposedly joined together by iron bolts and melted lead, as exposed at the base of a damaged column.

4.2 GPR investigations

This paragraph summarizes the main results of the GPR survey whereas a more in-depth analysis and discussion can be found in Nuzzo et al. (2005) and Masini et al. (2007). The GPR measurements were performed on different architectural elements of the rose window, along the external and internal façade (Fig. 1b), using a SIR2000 (GSSI) with 900 and 1500 MHz antennas in continuous mode. On the external side several consecutive profiles were carried out along the circular ashlar curb for a total length of about 20 m. Moreover, 11 radargrams were acquired along the intersecting arched ribworks and 11 radargrams along the columns. On the internal side, because of logistic problems, only the upper part of the circular ashlar curb (about 6 m) and some columns were investigated. Data processing includes horizontal scale normalization to a constant trace density, gain removal, time-zero correction, 1-D and 2-D filtering, background removal to enhance very shallow discontinuities, and Kirchhoff migration using a constant value of the electromagnetic wave velocity for each profile. The velocity was estimated by fitting diffractions to theoretical hyperbolas or using the reflection time from interfaces at known distance (typically the air interface beyond each architectural element).

Figure 3 (top) shows the 1500 MHz unmigrated radargrams related to two columns, A made of Pavonazzetto marble and B of grey breccia (right). Each radargram evidences three reflections referable to interfaces between the different materials (external column, inhomogeneous material, internal column). The columns are 10–11 cm thick and are separated by a 3–5 cm thick middle layer, where the carved panels are joined together by rubble and mortar, with possible voids accounting for the hyperbolas in the centre of radargram A. The semi-hyperbolas at the ends of the columns are attributed to the edges of iron anchor bolts linking the columns with the capital and penetrating inside the columns for about 5 cm (red arrows). The different building materials of the external columns reflect into a slightly different velocity value of the EM signal.

The middle section of Fig. 3 refers to the GPR survey on two arched ribworks (left and right pictures). The radargrams show anomalies related to visible (metallic bars -black arrows, fractures -blue lines), partially visible (restored blocks -rectangles, apparently extending for the whole thickness – CD – or just halfway – AB) and invisible features, such as metallic anchor bolts linking the intersecting arched ribworks with the capital or presumably joining a restored piece to the original part (green and yellow arrows) and the metallic tie-beams behind the rose window (brown). Although made of the same stone type (calcarenite), the different reflection amplitude of the left and right part of the air interface in radargram CD denotes the presence of two different materials in the two halves of the arched ribwork in terms of slightly different granulometry and/or water content.

The bottom part of Fig. 3 recapitulates the main GPR finding, namely the location of iron bolts (red and green) and fractures (blue), on the various elements of the rose window (left) and the GPR interpretation of the internal structure of the aslhar curb linking the rose window to the façade masonry (right). It is worth noting that, for the investigated columns (numbered in white), the iron anchor bolts have been detected at both ends, toward the capitals and the oculus, for the lower columns and only toward the capitals for the upper columns (Fig. 3 bottom-left).

The various processed radargrams acquired along the ashlar curb have been joined together and visualized as a single ring-like radargram (Fig. 3 bottom-right) to allow a better appreciation of the spatial relationships and facilitate the correlation with visible features of the curb masonry (e.g. the greenish sandstone ashlars). The composite GPR section highlights alternation of zones characterized by different propagation properties and reflection/diffraction patterns. There are three main discontinuous reflections. The first reflection at 4–5 ns (20–24 cm in depth, using an average

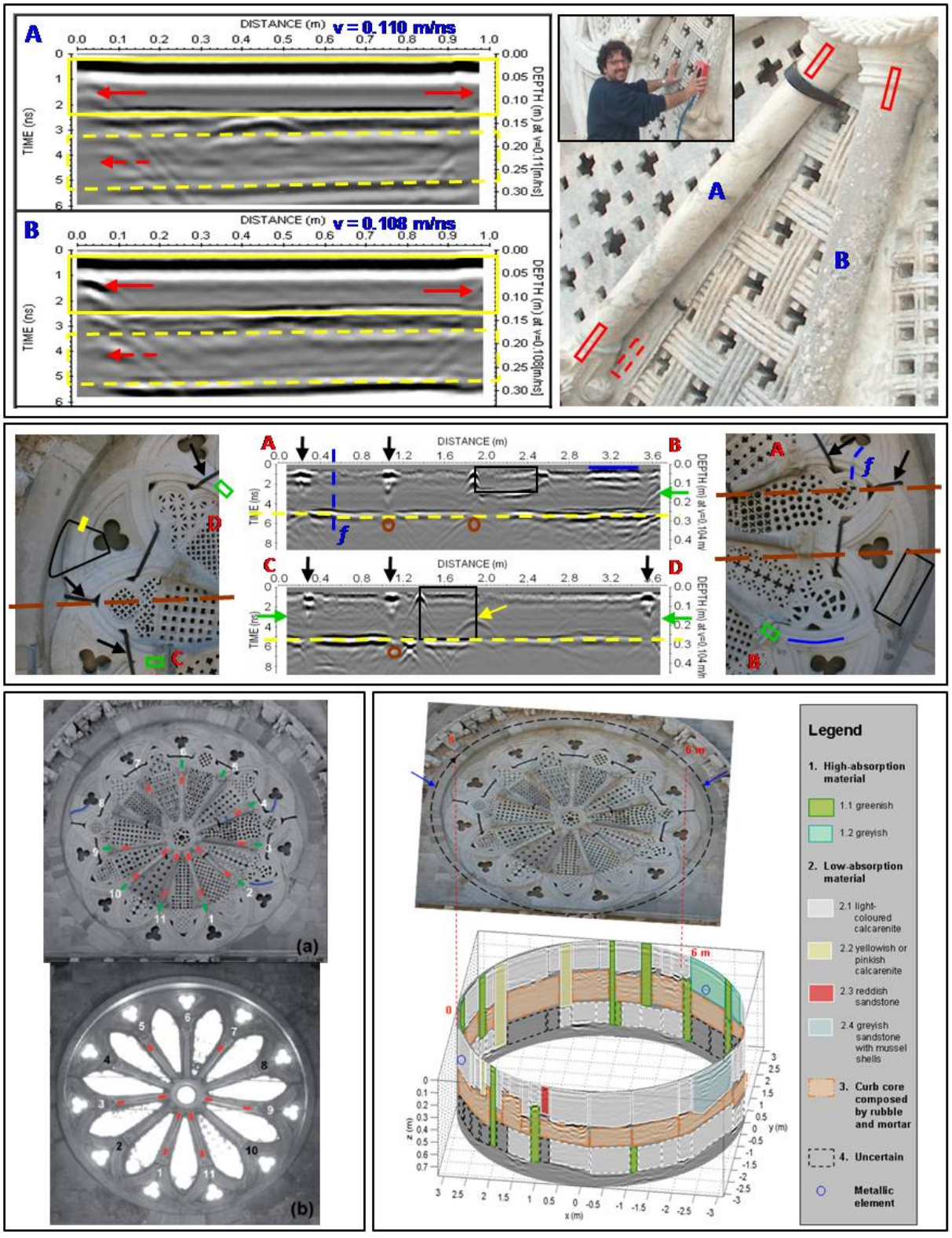

Fig. 3. Main results of the 1500 MHz GPR survey on the columns (top), intersecting arched ribworks (middle) and ashlar curb (bottom-right) with an overview of the GPR findings (fractures and iron bolts) inside the architectural elements of the rose window from the **(a)** external and **(b)** internal side of the façade (bottom-left) (see text for details).

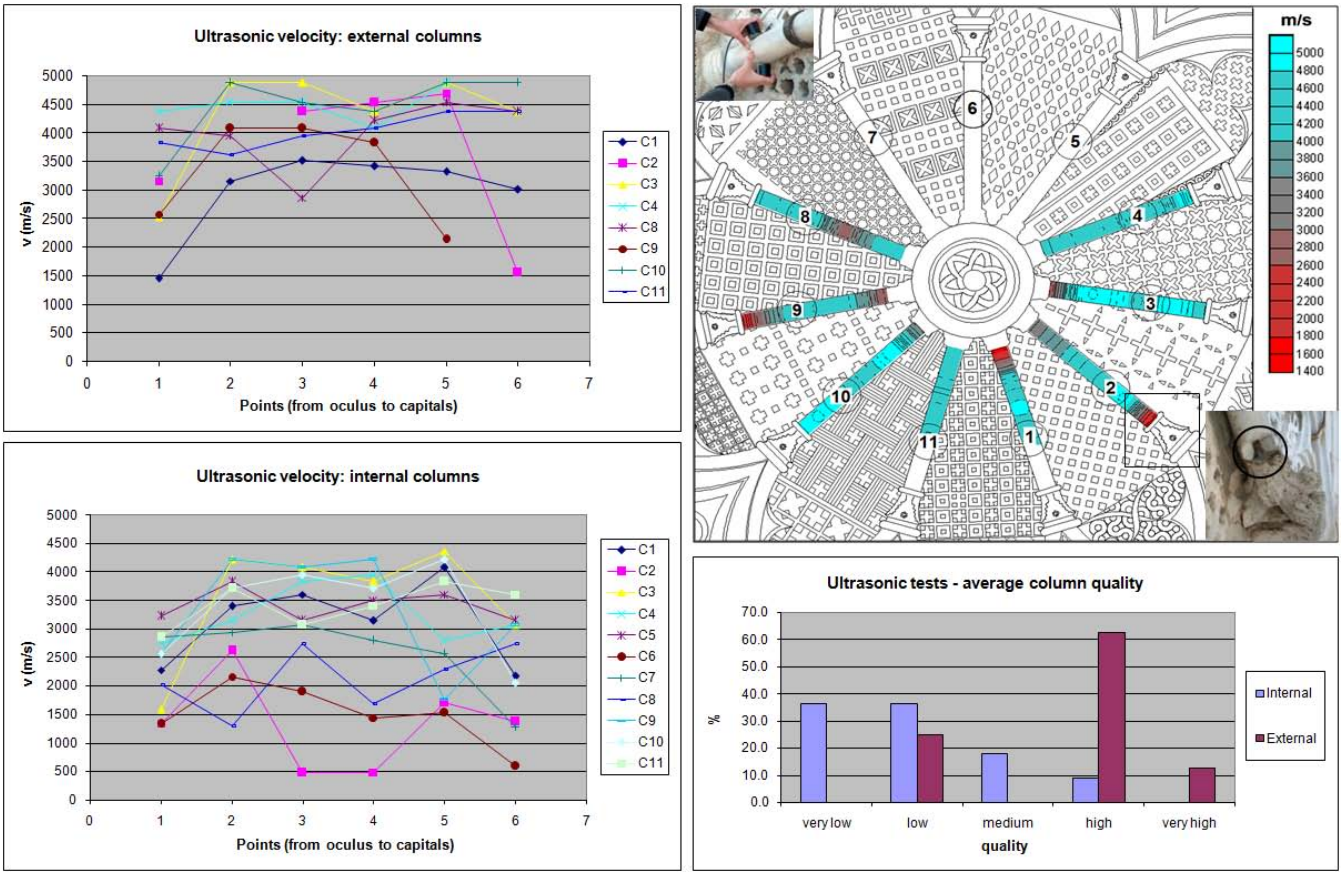

Fig. 4. (Left) Results of the ultrasonic tests on the external and internal columns. (Top-right) Ultrasonic velocity distribution on the external columns with (lower inset) example of low-velocity anomalies related to cracks or material detachment exposing a metallic anchor bolt. (Bottom-right) Column quality classification according to the ultrasonic results.

velocity of 0.098 m/ns) is followed by chaotic diffraction patterns revealing a heterogeneous material, probably rubble. The second reflection is recorded at depths of 40–45 cm and the final reflection is at about 65–66 cm. In some cases only the final reflection is recorded, probably due to the presence of monolithic ashlars, the so-called "diatons", inserted athwart in the masonry to connect the internal and the external rows of the curb (e.g. for those classified as material 2.2). In other zones no reflection is recorded because of the high absorption of the electromagnetic energy of some ashlars (e.g. for those classified as material 1.1). In most cases these high-absorption zones correlate well with the location of the greenish sandstone ashlars visible from the surface and are more abundant in the upper part of the rose window. In addition, two point-like diffractions (blue circles) are recorded inside the two largest ashlars close to the beginning of the overhanging sculptured arch (blue arrows), exactly where the main failures and rotational strains occurred. The absence of similar anomalies in the nearby arched ribworks suggests that these anomalies could be due to metallic anchor bolts connecting the curb to the external sculptured arch.

4.3 Ultrasonic tests

Ultrasonic tests have been carried out on the columns of the rose window and sonic tests on the arched ribworks. The sonic tests revealed no particular anomaly that could be related to architectural problems. Therefore only the results of the ultrasonic tests are presented. The ultrasonic survey was performed in direct transmission mode using a 2-channels, 24 bit MAE digital instrument (model A5000U) equipped with 55 kHz PUNDIT contact probes. For each column the acquisition was performed on six points, 20 cm spaced, from the oculus to the capital. On the external side, only the lower columns were investigated (Fig. 4 top-left and top-right). The tests showed a generally good ultrasonic velocity, generally ranging from 3000 to 5000 m/s (Table 1), apart for some local abrupt decreases probably related to localized damages. For instance, the low value of the mean ultrasonic velocity of column 1 is due to the extremely low value (1443 m/s) near the oculus related to local deterioration/cracking of the marble. This is corroborated by the similar velocity value (1552 m/s) measured on column 2 (made of the same material) close to the capital where the detachment of the upper

portion of marble has exposed the iron bolt connecting the column to the capital (lower inset of Fig. 4). Serious deterioration problems leading to material detachments affect also column 9, both near the oculus (see bottom of Fig. 5) and close to the capital. Another notable feature is the local velocity decrease in the middle of column 8 (and to a lower extent in the middle of column 4). This anomaly could be the visible expression of the location of the rotation axis during the past seismic event that caused the rose window to be displaced outwards in the upper part and inwards at the centre, but could also be related to additional (expulsive) strains induced by the metallic tie-beams running just behind them (dashed lines). The internal columns (Table 2) are characterized by a broader distribution of the velocity values with generally much lower average velocity (from about 1500 to 3500 m/s) than the external ones. This reflects the higher heterogeneity and apparently lower quality of the materials employed. In addition to localized defects, it is not excluded that some very low values of the ultrasonic velocity could have been caused by the loss of adhesion of the probes to the stone surface due to the thin plaster covering most of the internal columns.

In order to obtain a semi-quantitative quality classification of the columns based on the ultrasonic velocity, after eliminating the lowest velocity value (linked to defects or poor coupling) their mean velocity to standard deviation ratio has been calculated. Subsequently the columns have been divided into five groups according to a scale from 0 to 25 based on this parameter. In this way, as for their "defect-free" portion, it has been noticed that 5/8 (60%) of the external columns fall into the high-quality category, whilst 8/11 (70%) of the internal columns fall into the low and very-low quality groups (Fig. 4. bottom-right). This is not surprising as more precious materials (mainly reused marbles) have been used for the visible part of the façade and poorer materials (such as bricks and calcareous stones) for its hidden side. Finally, Table 3 summarizes the results of the ultrasonic survey and correlates the measured velocity with the column materials and observable state of decay.

4.4 IRT survey

Infrared thermography is a non-contact sensing method concerned with the measurement of radiated electromagnetic energy (the so called spectral radiance) emitted by a surface at a given temperature. The passive approach was adopted for the IRT survey on the rose window by performing the measurements on the external side exploiting the façade exposure to solar irradiation. Due to the façade orientation to the WNW, the survey was repeated for three consecutive days from late afternoon to evening. For each architectural element the thermal anomalies were verified through visual inspection and the analysis of high-resolution visible-light pictures. The IR system is an AVIO TVS-600 IR camera with Focal Plane Array detector operating in the "long wave" band (8–10 µm) where most of the objects at ambient temperature emit the maximum energy. The system has a thermal resolution of 0.15 °C and a spatial resolution of 14.0 mm × 13.7 mm at a recording distance of 10 m. Minimal image processing was applied to enhance subtle temperature variations. In Fig. 5 the most important thermal anomalies are compared with high-quality pictures, as well as GPR and ultrasonic results. Although the fracture evidenced by the IRT image is also well visible in the picture and clearly identifiable on the corresponding radargram (Fig. 5 middle), the presumable detachment (or the presence of a shallow iron bolt colder than the embedding stone) causing a subtle thermal decrease near the capital is hardly recognizable to the naked eye (Fig. 5 top). In addition the IRT technique was able to detect conservation treatments, such as the thermal anomaly related to the mortar-filled detachment near the joint between column 9 and the oculus that correlates well with the low-velocity value in the corresponding ultrasonic test (Fig. 5 bottom).

5 Structural diagnosis

The combination of direct observations and the analysis of the indirect, complementary information provided by the various non-destructive techniques allowed us to perform a detailed structural diagnosis of the monument and to reconstruct its construction stages and subsequent history. The main damage of the façade consists of a rotation around a horizontal "hinge", approximately 9.50 m above the base. The top of the façade is nearly 30 cm out of plumb. The origin of the rotation is clearly seismic, presumably a consequence of the 1731 earthquake, even though it is not possible to determine for certain the date and the intensity of the causative event.

The rotation is also confirmed by the displacement of the internal surface of the façade with reference to the corbel, which was originally located on the top of the longitudinal wall on the left of the central nave, with the aim to bear the first roof truss. That corbel was originally in contiguity with the internal surface of the façade wall, whilst now it is displaced of nearly 25 cm. The opening created by the rotation of the façade was closed in the past and the longitudinal walls were superelevated to prevent the interaction of the new roof trusses with the rose window. The new corbel, which presently bears the first roof truss, is in contiguity with the façade and is offset nearly 25 cm with reference to the original corbel below.

The damage of the façade is also confirmed by the damage of two couples of columns at the sides of the rose window (Fig. 1a). The columns on the right appear splintered, with damage especially pronounced for the column in red porphyry, which has also conchoid fractures in the upper part and in the capital. Both columns are slightly tilted towards the right and inwards. The couple of columns on the left

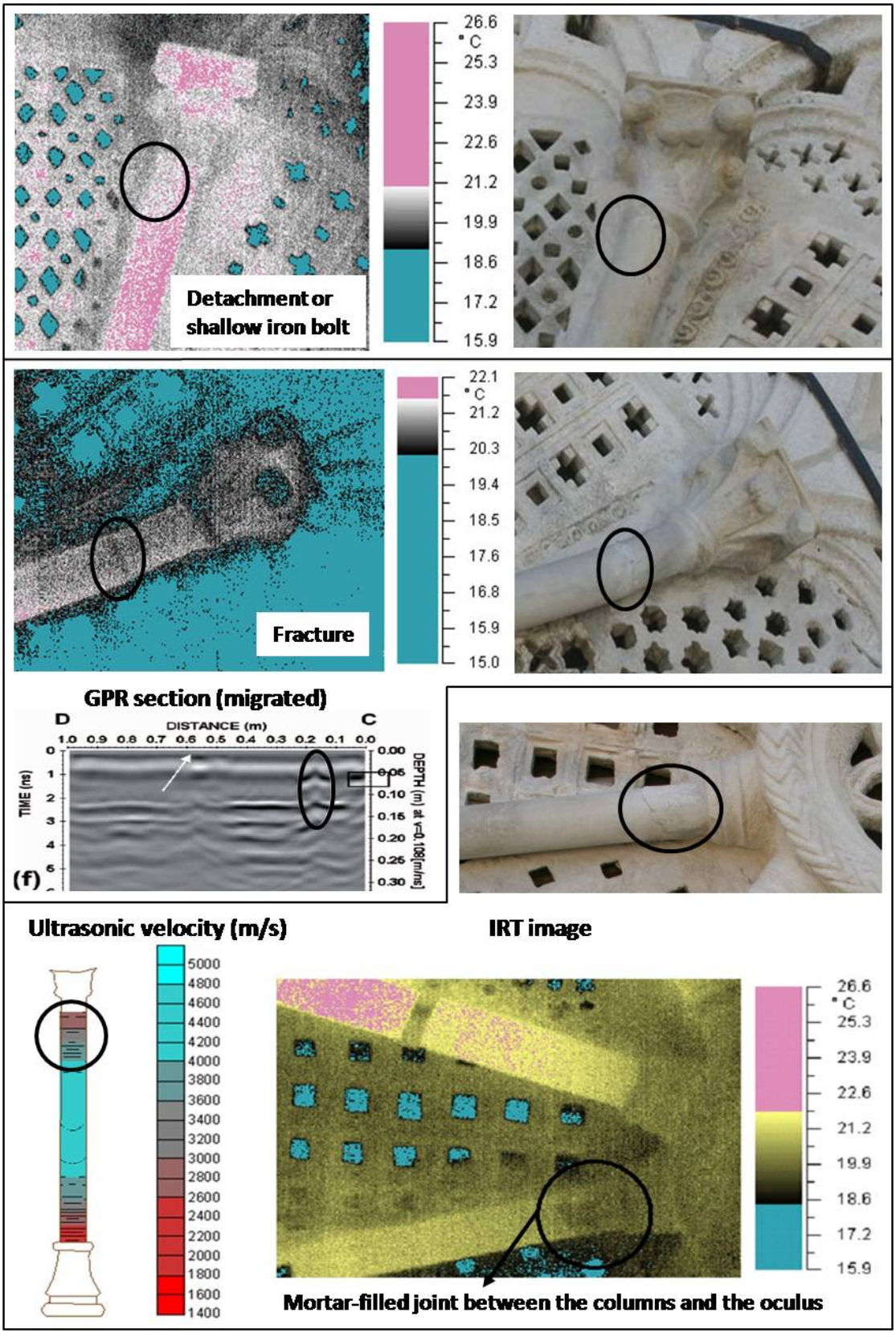

Fig. 5. Examples of IRT images and comparison with high-resolution photographs, 1500 MHz GPR investigations (middle) and ultrasonic tests (bottom).

Table 1. Ultrasonic tests on the external columns of the rose window.

Column	Material	Velocity measurements from oculus to capital v (m/s)						v min (m/s)	v max (m/s)	v mean (m/s)	Stand. dev. σ_v (m/s)
		Point 1	Point 2	Point 3	Point 4	Point 5	Point 6				
1	*Parian* Marble	1443	3155	3509	3413	3322	3003	1443	3509	2974	772
2	*Proconnesian* Marble	3155	/	4367	4525	4695	1552	1552	4695	3659	1325
3	Green-grey calcarenite	2519	4878	4878	4367	4878	4367	2519	4878	4314	914
4	*Proconnesian* Marble	4367	4525	4525	4082	4878	/	4082	4878	4475	289
5	Calcarenite										
6	*Pavonazzetto* Marble										
7	*Breccia Corallina*										
8	Calcarenite	4082	3953	2865	4219	4525	4367	2865	4525	4002	592
9	*Proconnesian* Marble	2571	4082	4082	3821	2132	/	2132	4082	3338	920
10	*Pavonazzetto* Marble	3236	4878	4525	4367	4878	4878	3236	4878	4460	638
11	Grey breccia	3831	3616	3953	4082	4367	4367	3616	4367	4036	299

Table 2. Ultrasonic tests on the internal columns of the rose window.

Column	Material	Velocity measurements from oculus to capital v (m/s)						v min (m/s)	v max (m/s)	v mean (m/s)	Stand. dev. σ_v (m/s)
		Point 1	Point 2	Point 3	Point 4	Point 5	Point 6				
1	*Proconnesian* Marble	2280	3400	3610	3155	4082	2173	2173	4082	3117	755
2	Calcareous stone	1350	2625	477	491	1721	1380	477	2625	1341	808
3	Calcareous stone	1585	4219	4082	3831	4367	3077	1585	4367	3527	1054
4	Calcareous stone	2740	3155	3831	3953	2801	3077	2740	3953	3260	516
5	*Proconnesian* Marble	3226	3831	3155	3509	3610	3155	3155	3831	3414	280
6	Bricks	1335	2169	1905	1443	1530	596	596	2169	1496	540
7	Calcareous stone	2865	2933	3077	2801	2571	1291	1291	3077	2590	658
8	Calcareous stone	2028	1307	2740	1698	2288	2740	1307	2740	2133	573
9	*Proconnesian* Marble	2571	4219	4082	4219	1770	3077	1770	4219	3323	1022
10	Calcareous stone	2570	3717	3953	3717	4219	2054	2054	4219	3372	857
11	Carrara Marble	2862	3717	3077	3413	3831	3610	2862	3831	3418	380

are tilted outwards and splintered at the base and at the top. Vertical cracks, indicating compression failure, can also be observed in their capitals.

The rotation of the façade is the presumable cause of a set of slidings and damages. The upper arch appears strongly ovalized; its keystone presents vertical fractures and is displaced outwards and downwards. The lower arch presents a vertical fracture at the key, and some voussoirs are displaced outwards and downwards.

The rotation of the façade induced heavy deformations and damages in the rose window, which is displaced outwards in the upper part and inwards at the centre. Disconnections and

Table 3. Synthesis of materials, decay and ultrasonic tests on the columns.

	Column	Material	Decay	Ultrasonic tests
External	1	*Parian* Marble	Fracture near the oculus	Low value at the joint with the oculus
	2	*Proconnesian* Marble	Rotation and cracks at column-capital joint	Low value at column-capital joint
	3	Green-grey calcarenite	Good preservation state	Generally rather high values, but low value near the oculus
	4	*Proconnesian* Marble	Fracture and shear dislocation near the joint	No measurement near the column-capital joint
	5	Calcarenite		
	6	*Pavonazzetto* Marble		
	7	*Breccia Corallina*		
	8	Calcarenite	Good preservation state	Excellent high velocity values, coherent with the good preservation state
	9	*Proconnesian* Marble	Fracture near the oculus	Low value near the oculus
	10	*Pavonazzetto* Marble	Good preservation state	Satisfactory velocity values with low standard deviation
	11	Grey breccia	Good preservation state	Satisfactory velocity values with low standard deviation
Internal	1	*Proconnesian* Marble	Compressive failure at column-capital joint	Low value at column-capital joint caused by the longitudinal crack
	2	Grey to green calcarenite	Strong decay at mid-length	Low values on the average, very low at mid-length
	3	Calcareous stone	Fracture near the oculus	Very high values for a calcareous stone, very low value near the oculus
	4	Calcareous stone	Rotation at column-capital joint, fracture near the oculus	High values for a calcareous stone, the lowest value is measured near the oculus
	5	*Proconnesian* Marble		Satisfactory values for a marble, the low standard deviation highlights homogeneous conditions
	6	Bricks		Very low values of the velocity
	7	Calcareous stone		Low value at column-capital joint
	8	Calcareous stone	Relative rotation at column-capital joint	Low value at measurement point 2 (40 cm from the oculus)
	9	*Proconnesian* Marble	Relative rotation at column-capital joint	
	10	Calcareous stone	Fracture at mid-length	
	11	Carrara Marble	Relative rotation at column-capital joint	

rotations of the capitals, as well as compression failures of the columns, may be observed. Relative displacements, up to 1 cm, may also be observed at the joints between the arched ribworks. An out-of-plane restraint was set up, presumably in the 19th century, consisting of two horizontal tubes, anchored to the ashlar curb and connected to some columns and arched ribworks through metal elements.

It is not clear whether this past intervention might have produced further strains to the anchoring architectural elements (such as in the middle of columns 8 and 4 and toward the oculus in columns 2 and 10) as suggested by the local decrease of ultrasonic velocity. This justifies their removal in future interventions, in favour of less invasive strengthening techniques. From a preliminary study, two different

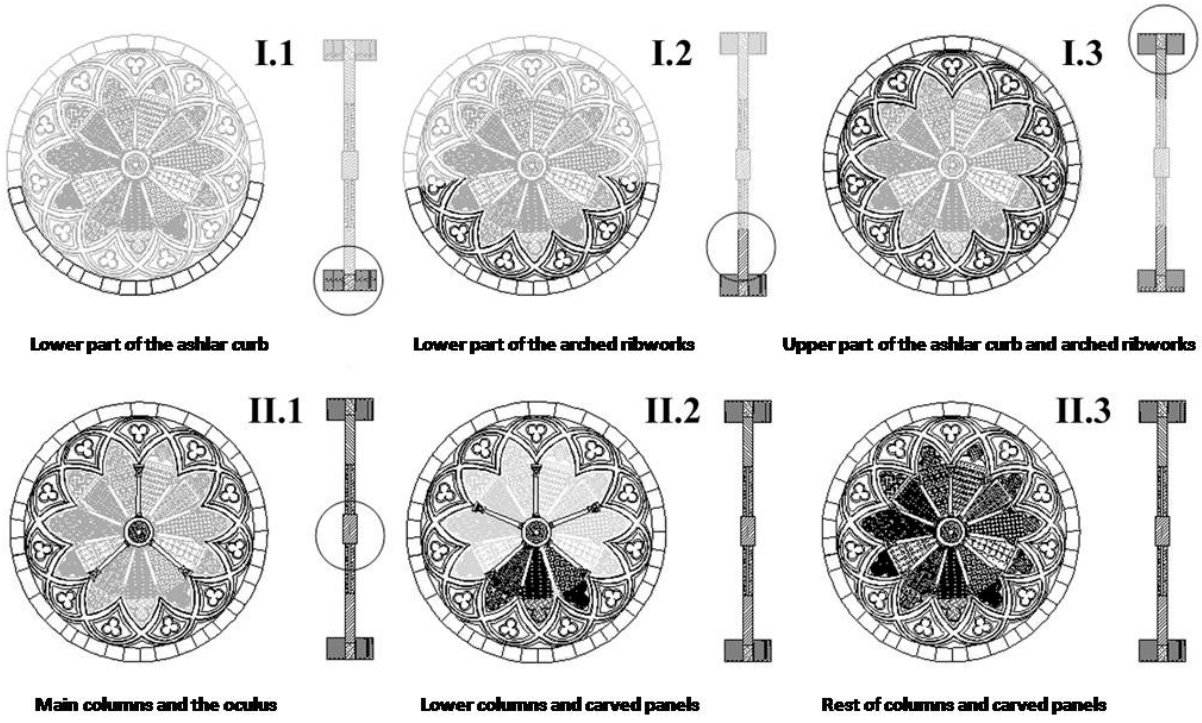

Fig. 6. Interpreted construction phases of the rose window of Troia Cathedral.

restoration techniques have been proposed: one consisting of dismantling the whole rose window followed by reassembly, the other involving an in situ structural reinforcement with partial dismantling of the architectural elements. To evaluate which method is preferable, besides a detailed knowledge of the materials and the present state of the internal structure, a comprehension is required of the original construction techniques. To this aim, the GPR results were invaluable to gain insights into the original construction techniques, and consequently select the restoration strategy more respectful of the original layout. In particular, the distribution of the iron bolts within the columns allowed us to discover the construction phases of the rose window. Based on the GPR findings, a hypothetical sequence of the construction stages is sketched in Fig. 6. After building the external ring (ashlar curb and arched ribworks), the columns, the central oculus and the carved panels were inserted. In the first phase the lower columns with iron bolts at both ends were positioned and the oculus was centred. Subsequently, the upper columns were inserted for some centimetres in the cups of the oculus and joined with the capitals by means of metal bolts. This solution permitted to optimize the tolerances during the positioning of the columns. The rose window was then completed with the insertion of the carved panels. The GPR investigation provided crucial evidences in favour of one of the various conflicting hypotheses about the original construction techniques, leading to the selection of partial dismantling as the most suitable restoration strategy.

6 Conclusions

This case study demonstrates the effectiveness of integrated non destructive techniques in the study of Architectural Heritage for the assessment of the state of preservation of the monument and its material and construction components, which is essential to addressing maintenance and restoration issues.

The rose window of Troia Cathedral presents a set of damages and deformations of seismic origin which can be ascribed to a rotation of the façade around a horizontal hinge passing through the centre of the rose window. With the aim to set up the most suitable restoration intervention, a series of diagnostic investigations have been carried out: identification of the materials, GPR prospecting, sonic and ultrasonic tests, infrared termography.

The GPR survey provided fundamental information on the internal structure and state of preservation of the rose window. It enabled the determination of the internal structure of the circular ashlar curb and detected cracks in the columns and calcarenite elements with intersecting arches, as well as the boundaries between original and restored parts. Moreover, it enabled the localization of iron bolts in joints between columns and capitals, and between columns and central oculus, providing useful insights into the original construction techniques which were essential to evaluate the feasibility of the planned restoration strategy. Ultrasonic tests were useful to detect low-velocity zones inside the columns, related to

various kinds of decay. In addition, they enabled the determination of the elastic modulus useful for the assessment of the mechanical properties of the investigated structures. Passive IRT was a fast and relatively cheap technique for detecting shallow defects (cracks and superficial metal elements) and past conservation treatments (mortar-filled voids).

This multi-scale integrated investigation proved to be a successful diagnostic strategy to tackle the problem of detecting features at different scales, ranging from the sub-centimetre size of small metal joints, narrow fractures and thin mortar fillings, up to the sub-metre scale of the masonry structure of the circular ashlar curb linking the rose window to the façade. The non destructive multi-technique approach provided a wide amount of high-resolution complementary information on the internal and surface characteristics, materials, state of conservation and construction techniques, which are essential to design an effective restoration strategy.

Acknowledgements. This study has been funded by Comune di Troia and Ente Diocesi di Lucera-Troia. The authors are also grateful to Edoardo Beccia, Stefano Cibelli, Piero Guadagno and Giulio Tricarico for their help.

Edited by: L. Eppelbaum, N. Masini, and F. Soldovieri
Reviewed by: two anonymous referees

References

Avdewlidis, N. P. and Moropolou, A.: Applications of infrared thermography for the investigation of historical structures, J. Cult. Herit., 5, 119–127, 2004.

Belli D'Elia, P.: Per la storia di Troia: dalla chiesa di S. Maria alla cattedrale, Vetera Christianorum, 25, 605–620, 1998.

Binda, L., Lenzi, G., and Saisi, A.: NDE of masonry structures: use of radar tests for the characterisation of stone masonries, NDT & E International, 31(6), 411–419, 1998.

Binda, L., Saisi, A., and Tiraboschi, C.: Application of sonic tests to the diagnosis of damaged and repaired structures, NDT & E International, 34(2), 123–138, 2001.

Binda, L., Saisi, A., Tiraboschi, C., Valle, S., Colla, C., and Forde, M.: Application of sonic and radar tests on the piers and walls of the Cathedral of Noto, Constr. Build Mater., 17(8), 613–627, 2003(a).

Binda, L., Saisi, A., and Zanzi, L.: Sonic tomography and flat-jack tests as complementary investigation procedures for the stone pillars of the temple of S. Nicolò l'Arena (Italy), NDT & E International, 36(4), 215–227, 2003(b).

Binda, L., Zanzi, L., Lualdi, M., and Condoleo, P.: The use of georadar to assess damage to a masonry Bell Tower in Cremona, Italy, NDT & E International, 38(3), 171–179, 2005.

Borghini, G. (cura di): Marmi antichi, Roma, 1989.

Calia, A., Giannotta, M. T., and Quarta, G.: A contribution to the study of re-used architectural marbles in Troia Cathedral (Foggia province, Southern Italy): identification and determination of provenance, in Marbres et autres roches de la Méditerranée antique: études interdisciplinaires, Proceed. VIIIth Asmosia Int. Conf., Aix-en-Provence, 739–758, 2006.

Cardarelli, E., Godio, A., Morelli, G., Sambuelli, L., Santarato, G., and Socco L. V.: Integrated geophysical surveys to investigate the Scarsella vault of St. John's Baptistery in Florence, The Leading Edge, 67, 467–470, 2002.

Cataldo, R., De Donno, A., De Nunzio, G., Leucci, G., Nuzzo, L., and Siviero, S.: Integrated methods for analysis of deterioration of cultural heritage: the Crypt of "Cattedrale di Otranto", J. Cult. Herit., 6, 29–38, 2005.

Clark, M. R., McCann, D. M., and Forde, M. C.: Application of infrared thermography to the non-destructive testing of concrete and masonry bridges, NDT & E International, 36(4), 265–275, 2003.

Colla, C., Das, P. C., McCann, D., and Forde, M. C.: Sonic, electromagnetic and impulse radar investigation of stone masonry bridges, NDT & E International, 30(4), 249–254, 1997.

Dunham, R. J.: Classification of carbonate rocks according to depositional texture. Classification of carbonate rocks. Mem. American Association Petrology and Geology, 1, W.E. Ham Ed., 108–121, 1962.

Flint, R. C., Jackson, P. D., and McCann, D. M.: Geophysical imaging inside masonry structures, NDT & E International, 32(8), 469–479, 1999.

Folk, R. L.: Practical petrographic classification of limestones, Am. Assoc. Petr. Geol. B., 43, 1–38, 1959.

Gnoli, R: Marmora Romana, Roma, 1971.

Grinzato, E., Bison, P. G., and Marinetti, S.: Monitoring of ancient buildings by the thermal method, J. Cult. Herit., 3, 21–29, 2002.

Inagaki, T., Ishii, T., and Iwamoto, T.: On the NDT and E for the diagnosis of defects using Infrared thermography, NDT&E International 32, 247–257, 1999.

Liberatore, D., Spera, G., Mucciarelli, M., Masini, N., Calia, A., Capriuoli, A., Racina, V., Nuzzo, L., Rizzo, E., Binda, L., and Cantini, L.: The façade and the rose-window of Troia Cathedral (Apulia, Italy). Structural Analysis of Historical Constructions, edited by: Lourenço, P. B., Roca, P., Modena, C., and Agrawal, S., ISBN 972-8692-27-7, New Delhi, 2006.

Maierhofer, C. and Leipold, S.: Radar investigation of masonry structures, NDT & E International, 34, 139–147, 2001.

Maierhofer, C., Brink, A., Röllig, M., and Wiggenhauser, H.: Detection of shallow voids in concrete structures with impulse thermography and radar, NDT & E International, 36 (4), 257–263, 2003.

Masini, N., Nuzzo, L., and Rizzo, E.: GPR investigations for the study and the restoration of the Rose Window of Troia Cathedral (Southern Italy), Near Surf. Geophys., 5, 287–300, 2007.

Masini, N., Persico, R., and Rizzo, E.: Some Examples of GPR Prospecting for Monitoring of the Monumental Heritage, Journal Geophysics Engineering, 7, 1–10, 2010.

McCann, D. M. and Forde, M. C.: Review of NDT methods in the assessment of concrete and masonry structures, NDT & E International, 34 (2), 71–84, 2001.

Nuzzo, L., Leucci, G., and Negri, S.: GPR, ERT and magnetic investigations inside the Martyrium of St Philip, Hierapolis, Turkey, Archaeol. Prospect., 16(3), 177–192, 2009.

Nuzzo, L., Leucci, G., Negri, S., Carrozzo, M. T., and Quarta, T.: Application of 3D visualization techniques in the analysis of GPR data for archaeology, Ann. Geophys.-Italy, 45(2), 321–337, 2002.

Nuzzo, L., Masini, N., Rizzo E., and Lasaponara, R.: Integrated

and multiscale NDT for the study of architectural heritage Proc. SPIE Vol. 7110, Remote Sensing for Environmental Monitoring, GIS Applications and Geology VIII, edited by: Michel, U., Civco, D. L., Ehlers, M., and Kaufmann, H. J., 711015, doi:10.1117/12.801313, 2008.

Nuzzo, L., Rizzo, E., and Masini, N.: Georadar investigations for the diagnosis of the rose window of the cathedral of Troia (Southern Italy): preliminary results, Proceedings of Art'05 – 8th Int. Conf. on "Non Destructive Investigations and Micronalysis for the Diagnostics and Conservation of the Cultural and Environmental Heritage" Lecce (Italy), May 15–19, 2005.

Ranalli, D., Scozzafava, M., and Tallini, M.: Ground penetrating radar investigations for the restoration of historic buildings: the case study of the Collemaggio Basilica (L'Aquila, Italy), J. Cult. Herit., 5, 91–99, 2004.

Titman, D. J.: Applications of thermography in non-destructive testing of structures, NDT & E International, 34(2), 149–154, 2001.